Load Carrying Mechanism of Concrete Beams Restrained Externally by Steel Plates

Ryo Matsumoto[1], Toshiki Muranishi[2], Hiroaki Kitoh[3] and Masayuki Nakabayashi[4]

[1] Osaka City University, Osaka, Japan, ryo1814321@gmail.com
[2] Tokyo Metropolitan Government, Tokyo, Japan, Toshiki_Muranishi@member.metro.tokyo.jp
[3] Osaka City University, Osaka, Japan, kitoh@civil.eng.osaka-cu.ac.jp
[4] CORE Institute of Technology Corp., Osaka, Japan, nakabayashi@coreit.co.jp

Abstract
Compressive Membrane Action: CMA is a well-known load carrying mechanism of slabs due to external restraint. We have conducted three concrete beam loading test having an existence of external restraint and corresponding material nonlinear finite element analyses in order to reveal the compressive strut mechanism in the beam as a preliminary and approach of compressive membrane action. The validity of the numerical method employed herein can be verified so sufficiently that we could show clearly a compressive strut formation and also its load carrying mechanism with a steel plate in tension.
Keywords: External Restraint, Compressive Strut, Beam Model Test, Non-linear Finite Element Method

1. INTRODUCTION

Compressive Membrane Action: CMA is a well-known load carrying mechanism of slabs due to external restraint [1], which is also called compressive dome or truss action in beam members. The action has been introduced effectively into the roadway design codes in the United Kingdom [2] and North America [3]. As a countermeasure of salt attack into reinforced concrete slab decks, steel free bridge decks incorporated CMA, furthermore, have been constructed in Canada [4] and the United States provided steel straps connecting between adjacent top flanges of steel main girders restraining externally concrete slabs as shown in Fig. 1. We pay a fundamental attention to the two-dimensional action, so that, load carrying mechanism of concrete beams restrained by steel plate have been examined experimentally and also numerically.

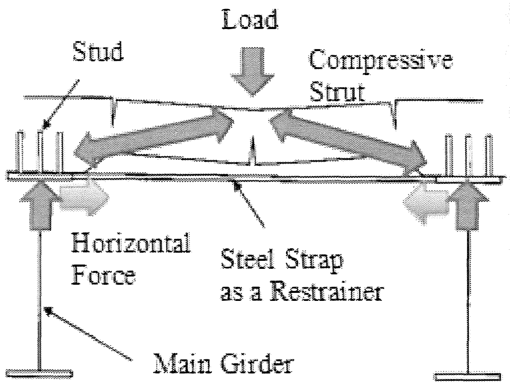

Fig. 1 Compressive Membrane Action in Concrete Slabs of Composite Girder Bridge

2. EXPERIMENT METHOD

Table 1 indicates the parameters and concrete beam specimens having their combination, in which the first is an existence of external restraint and the second is that of reinforcement. A specimen without the restraint and also the reinforcement is just a flexural concrete test specimen to fail at flexural crack initiation. We prepared, thus, three specimens in Table 1. The dimensions of all the specimens were identical as 120mm breadth, 210mm height and 2140mm long. A steel strap of 12mm thick was used as a restrainer and connected to a concrete beam by 12 headed studs with 6mm diameter and 100mm height. SF is a target specimen as shown in Fig.1. NR is a conventional reinforced concrete one designed to cause flexural failure. Compressive strength of concrete and yield point of the steel plate was 55N/mm^2 and 290N/mm^2, respectively. Tensile and compressive reinforcement ratio was 1.28% and 0.72%, respectively. A patch load relevant to a wheel load was given at the center of each specimen's top surface. Furthermore, a chloroprene rubber and a steel plate were inserted between the surface of concrete and loading cross-head. We observed the load intensity, mid-span deflection, crack development, concrete surface and re-bar strains up to failure.

Table 1 Specimen and Parameters

Tag	External Restraint	Steel Reinforcement
NR		✓
SR	✓	✓
SF	✓	

3. NUMERICAL METHOD

We have carried out two-dimensional material non-linear finite element analyses [5] with respect to all the specimens. Plane stress elements were used for concrete beam and steel strap, while truss elements were used for reinforcement. The relation between shear force and slip of stud connectors was also considered.

4. RESULTS and DISCUSSION

4.1 Experimental Results

First, the maximum load of specimen NR and SR was 33.0 and 193.0kN, respectively. It can be said that the external restrainer caused 5.8 times enhancement of the maximum load. Moreover, the load of specimen SF was 93.5kN. To compare SR with SF, the maximum load doubled owing to reinforcement. Second, cracking loads are essential for serviceability limit state. The load of NR, SR and SF was 7.0, 19.0 and 13.0kN, respectively. As the same manner of the maximum load, the cracking load increased 2.7 times owing to the external restrainer. Furthermore, the cracking load of SR also increased 1.5 times as that of SF. Thus, such the enhancement due to an existence of the strap could suggest the effect of the compressive strut contribution. As to the crack distribution, first, the distribution of SR was similar to that of NR in narrow portion around mid-span, however, other flexural cracks also observed on top surface expanding downward at both supporting portions. It could be considered that hogging moment due to external restraint caused the latter cracks. Second, as shown in Fig. 2, the cracks of SF were a few and locally, then opened considerably owing to no reinforcement. Moreover, the potion of crack was as same as that of SR partially under hogging moment, which cracks expanded downwards.

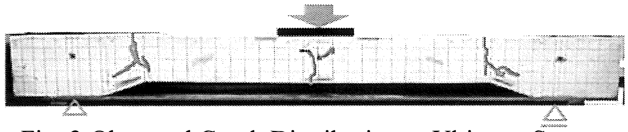

Fig. 2 Observed Crack Distribution at Ultimate State of SF

4.2 Numerical Results

The cracks of NR of SR obtained numerically have good agreements with the experiment result as mentioned in 4.1. However, as shown in Fig.3, the mid-span cracks were recognized to be distributed, differing from the observed result as shown in Fig.2. We employed the smeared crack model, which was inferior to discrete crack model expressing such a behavior. Next, as to the minimum principal stress distributions in concrete at ultimate state, the aspect of NR without the strap was as an ordinary beam mechanism. The rest of two with the strap, for example as shown in Fig. 4, however, were essential difference, in which one can be seen arch shaped compressive zones connecting a support through the loading portion to another support as shown in Fig.1. It can be suggested the formation of compressive strut due to external restraint of the strap.

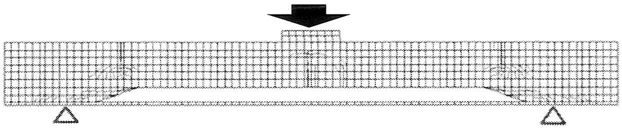

Fig. 3 Crack Distribution Obtained Numerically of SF

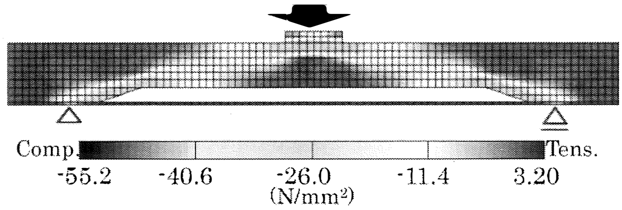

Fig. 4 Minimum Principal Stress Distribution at Ultimate State of SF

4.3 Verification

Fig. 5 shows comparison of the load-mid span deflection relations between experiment and numerical results for all the specimens, in which important occurrences of initial cracking, tensile and compressive re-bars yielding are also indicated. As to both NR and SR, the relations and also the occurrences can show a satisfactory agreement. The relation of SF obtained numerically was slightly overestimated to the experimental results, though its occurrence can be predicted well. It can be considered that the smeared crack model mentioned above caused the relation's difference. Thus, the validity of the numerical method employed herein can be verified so sufficiently that .we could show clearly compressive strut formation and also its load carrying mechanism with a steel strap in tension.

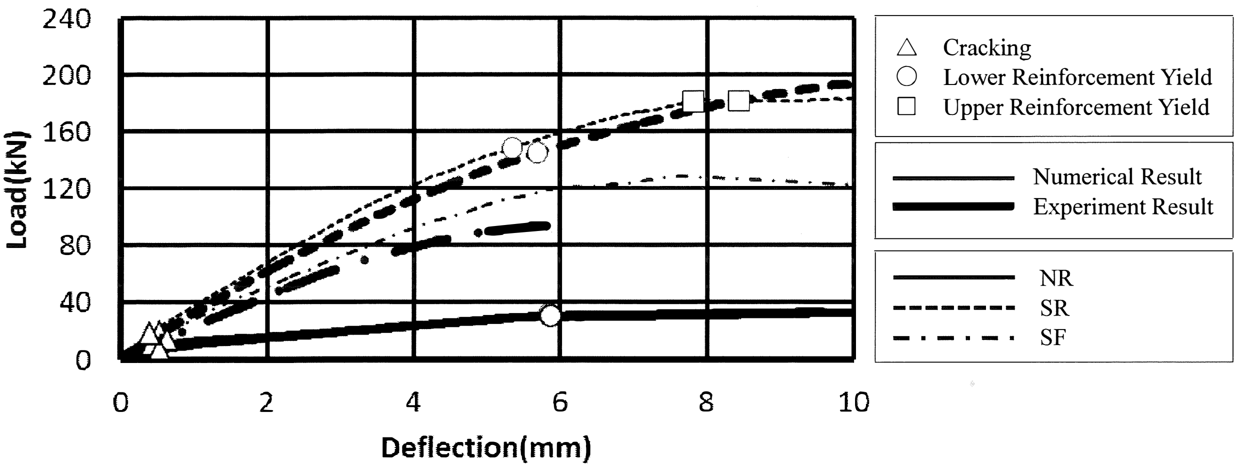

Fig. 5 Deflection Load Relations

5. REFERENCES

[1] Ockleston, A.J., The Structural Engineers, Vol. 33, pp.304-322, 1955. [2] United Kingdom Highway Agency, Design Manual for Roads and Bridges, Vol. 3, Section 4, Part 20, BD81/02, 2002. [3] Baidar Bakht et al., Journal of Composites for Construction, ASCE, Vol. 4, No. 1, pp.3-15, 2000. [4] John P. Newhook et al., Concrete International, Vol. 18, pp.30-34, 1996. [5] Obayashi Co. Technical Research Institute, "*Final Theory Manual*", 2011.